Inorg. Chem. **2007**, *46*, 9655–9660

S K-Edge XAS and DFT Calculations on Square-Planar Ni^{II}–Thiolate Complexes: Effects of Active and Passive H-Bonding

Abhishek Dey,[†] Kayla N. Green,[§] Roxanne M. Jenkins,[§] Stephen P. Jeffrey,[§] Marcetta Darensbourg,*[,§] Keith O. Hodgson,*[,†,‡] Britt Hedman,*[,‡] and Edward I. Solomon*[,†,‡]

Department of Chemistry, Stanford University, Stanford, California 94305, Stanford Synchrotron Radiation Laboratory, SLAC, Stanford University, Menlo Park, California 94025, and Department of Chemistry, Texas A&M University, College Station, Texas 77843

Received April 3, 2007

S K-edge XAS for a low-spin Ni^{II}–thiolate complex shows a 0.2 eV shift to higher pre-edge energy but no change in Ni–S bond covalency upon H-bonding. This is different from the H-bonding effect we observed in high-spin Fe^{III}–thiolate complexes where there is a significant decrease in Fe–S bond covalency but no change in energy due to H-bonding (Dey, A.; Okamura, T.-A.; Ueyama, N.; Hedman, B.; Hodgson, K. O.; Solomon, E. I. *J. Am. Chem. Soc.* **2005**, *127*, 12046–12053). These differences were analyzed using DFT calculations, and the results indicate that two different types of H-bonding interactions are possible in metal–thiolate systems. In the high-spin Fe^{III}–thiolate case, the H-bonding involves a thiolate donor orbital which is also involved in bonding with the metal (active), while in the low-spin Ni^{II}–thiolate, the orbital involved in H-bonding is nonbonding with respect to the M–S bonding (passive). The contributions of active and passive H-bonds to the reduction potential and Lewis acid properties of a metal center are evaluated.

Introduction

Hydrogen bonding plays an important role in tuning the reactivity of protein active sites by modulating active-site geometric and electronic structure.[1,2] The role of these H-bonds has been evaluated using several different experimental and computational techniques.[3,4] Although there are some significant developments in understanding H-bonding with second-row elements (N, O, etc.), only a few studies have evaluated the effects of H-bonding on the structure and reactivity of inorganic complexes and active sites having sulfur ligands.[5−9] Metal−sulfur-based active sites are abundant in nature, performing a wide variety of functions, including redox catalysis (e.g., O_2 activation by cytochrome P450), small-molecule activation (e.g., superoxide reductase), Lewis acid catalysis (e.g., nitrile hydratase), and electron transport (e.g., Fe−S and blue copper proteins).[10−13] Many of these sites have multiple H-bonding interactions between the sulfur ligands (thiolates or bridging sulfides atoms) and the peptide backbone. These active sites significantly differ in electronic structure relative to geometrically similar

* To whom correspondence should be addressed. E-mail: Edward.Solomon@stanford.edu.
[†] Department of Chemistry, Stanford University.
[‡] Stanford Synchrotron Radiation Laboratory, SLAC, Stanford University.
[§] Department of Chemistry, Texas A&M University.

(1) Steiner, T. *Angew. Chem., Int. Ed.* **2002**, *41*, 48−76.
(2) Hobza, P.; Havlas, Z. *Chem. Rev.* **2000**, *100*, 4253−4264.
(3) (a) Kumar, G. A.; Pan, Y. P.; Smallwood, C. J.; McAllister, M. A. *J. Comput. Chem.* **1998**, *19*, 1345−1352. (b) Francois, S.; Rohmer, M. M.; Benard, M.; Moreland, A. C.; Rauchfuss, T. B. *J. Am. Chem. Soc.* **2000**, *122*, 12743−12750.
(4) (a) Lipscomb, W. N.; Strater, N. *Chem. Rev.* **1996**, *96*, 2375−2433. (b) Bhaumik, D.; Medin, J.; Gathy, K.; Coleman, M. S. *J. Biol. Chem.* **1993**, *268*, 5464−5470. (c) Sideraki, V.; Mohamedali, K. A.; Wilson, D. K.; Chang, Z.; Kellems, R. E.; Quiocho, F. A.; Rudolph, F. B. *Biochemistry* **1996**, *35*, 7862−7872.
(5) Yang, X.; Niu, S. Q.; Ichiye, T.; Wang, L. S. *J. Am. Chem. Soc.* **2004**, *126*, 15790−15794.
(6) Torres, R. A.; Lovell, T.; Noodleman, L.; Case, D. A. *J. Am. Chem. Soc.* **2003**, *125*, 1923−1936.
(7) (a) Ueno, T.; Ueyama, N.; Nakamura, A. *J. Chem. Soc., Dalton Trans.* **1996**, *19*, 3859−3863. (b) Ueyama, N.; Yamada, Y.; Okamura, T.; Kimura, S.; Nakamura, A. *Inorg. Chem.* **1996**, *35*, 6473−6484.
(8) Hung, W. P.; Dewan, J. C.; Tuckerman, M.; Walters, M. A. *Inorg. Chim. Acta* **1999**, *291*, 388−394.
(9) Huang, J.; Dewan, J. C.; Walters, M. A. *Inorg. Chim. Acta* **1995**, *228*, 199−206.
(10) Meunier, B.; de Visser, S. P.; Shaik, S. *Chem. Rev.* **2004**, *104*, 3947−3980.
(11) (a) Lee, S. C.; Holm, R. H. *Chem. Rev.* **2004**, *104*, 1135−1157. (b) Rao, P. V.; Holm, R. H. *Chem. Rev.* **2004**, *104*, 527−559.
(12) Endo, I.; Nojiri, M.; Tsujimura, M.; Nakasako, M.; Nagashima, S.; Yohda, M.; Odaka, M. *J. Inorg. Biochem.* **2001**, *83*, 247−253.
(13) Rorabacher, D. B. *Chem. Rev.* **2004**, *104*, 651−697.

10.1021/ic7006292 CCC: $37.00
Published on Web 10/20/2007

inorganic model complexes. H-bonding interactions can affect the M−S bond covalency and thus make a significant contribution to the observed large differences in reactivity between model complexes and protein active sites.[14] However, current knowledge about these relatively weak yet crucial interactions is limited by the fact that conventional spectroscopic techniques are often not very sensitive to the small perturbation of H-bonding.

Ligand K-edge X-ray absorption spectroscopy (XAS) is a powerful physical method that provides a direct experimental estimate of the covalency of metal−ligand bonds.[15,16] The K-edge XAS spectrum of a ligand bound to a transition metal can have an intense *pre-edge* feature. This is assigned to the ligand 1s-(L_{1s})-to-metal-based 3d (M_{3d}) transition. The intensity of this transition is directly proportional to the percent ligand np character (in this case, percent S_{3p}) mixed into unoccupied or half-occupied metal-based 3d orbitals of the ground-state wavefunction (Ψ) of the transition-metal complex.

$$\Psi = (1 - \alpha^2)^{1/2}|M_{3d}> + \alpha|L_{np}> \quad (1)$$

where α is the ligand coefficient in the half-occupied or unoccupied orbital. The intensity (I) of the $L_{1s} \rightarrow M_{3d}$ transition is

$$I(L_{1s} \rightarrow M_{3d}) = \alpha^2 I(L_{1s} \rightarrow L_{np}) \quad (2)$$

where $I(L_{1s} \rightarrow L_{np})$ is the intensity of a purely ligand-based $1s \rightarrow np$ transition, which depends primarily on the Z_{eff} value of the ligand.[17] The pre-edge intensity thus provides a direct estimate of ligand−metal bond covalency (α^2). Due to the localization of the core hole on the ligand, this technique involves minimal final state effects (e.g., core hole interaction with the d^{n+1} final state) and electronic relaxation.[17]

This technique has previously been used to investigate the effect of H-bonding in active sites of Cu−S and Fe−S electron-transfer proteins.[15,18] XAS data on the proteins showed significant reductions of M−S bond covalency, which qualitatively correlated to the extent of H-bonding interaction in the active site.[19−21] For a quantitative estimate of this effect, S K-edge XAS on a series of heme thiolate model complexes was performed where the H-bonding to the thiolate ligand was systematically increased.[22] The data showed dramatic reduction in pre-edge intensity with increasing H-bonding, which indicated the weakening of Fe−S $d\pi-p\pi$ covalency. The increased H-bonding was calculated to stabilize the reduced site more than the oxidized state, which predicts a positive shift in the reduction potential, as experimentally observed.

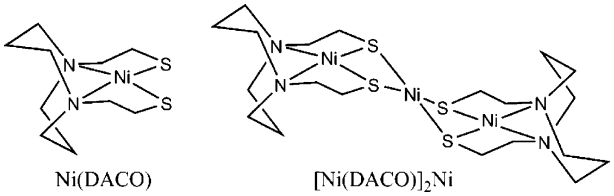

Figure 1. Schematic representation of Ni(DACO) and $[Ni(DACO)]_2Ni$ complexes used in this study.

In this study, we report S K-edge XAS and density functional theory (DFT) calculations on square-planar Ni^{II}−thiolate complexes (Figure 1) as solids and in H-bonding solvent solutions. The data obtained here show a very different behavior than the experimental results we observed in ref 22 for the heme thiolate system; there is no decrease in Ni−S bond covalency but there is a shift in pre-edge energy due to H-bonding. DFT calculations reproduce this behavior and indicate that it is the result of the differences in M−S bonding interactions between a thiolate and a high-spin d^5 Fe^{III} ion which involves π and σ bonds and a low-spin d^8 Ni^{II} ion which involves only σ bonds. This reflects two very different types of H-bonding scenarios having similar overall energy but rather different effects on electronic structure.

Experimental Details

Materials and Methods. The complexes Ni^{II}[*N*,*N*′-bis(2-mercaptoethyl)-1,5-diazacyclooctanato] (Ni(DACO)) and Ni^{II}[bis-Ni^{II}-[*N*,*N*′-bis(2-mercaptoethyl)-1,5-diazacyclooctanato]] ($[Ni(DACO)]_2Ni$) were synthesized as described in ref 23. Dry acetonitrile (percent $H_2O \ll 0.01\%$) was obtained from Acros. For XAS experiments, the samples were ground into a fine powder and dispersed as thinly as possible on sulfur-free Mylar tape. This procedure has been verified to minimize self-absorption effects. The sample was then mounted across the window of an aluminum plate. Fresh solutions of Ni(DACO) and $[Ni(DACO)_2Ni]$ were prepared before the experiments ~10 mM in concentration. The solutions were loaded via a syringe into a Pt-plated Al block sample holder sealed in front using a 6.3 μm polypropylene window and maintained at a constant temperature of 4 °C during data collection using a controlled flow of N_2 gas precooled by liquid N_2 passing through an internal channel in the Al block.

Data Collection. XAS data were measured at the Stanford Synchrotron Radiation Laboratory using the 54-pole wiggler beam line 6-2. Details of the experimental configuration for low-energy studies have been described previously.[16] The energy calibration, data reduction, and error analysis follow the methods described in ref 16.

(14) Stephens, P. J.; Jollie, D. R.; Warshel, A. *Chem. Rev.* **1996**, *96*, 2491−2513.
(15) Glaser, T.; Hedman, B.; Hodgson, K. O.; Solomon, E. I. *Acc. Chem. Res.* **2000**, *33*, 859−869.
(16) Solomon, E. I.; Hedman, B.; Hodgson, K. O.; Dey, A.; Szilagyi, R. K. *Coord. Chem. Rev.* **2005**, *249*, 97−129.
(17) Neese, F.; Hedman, B.; Hodgson, K. O.; Solomon, E. I. *Inorg. Chem.* **1999**, *38*, 4854−4860.
(18) Solomon, E. I.; Gorelsky, S. I.; Dey, A. *J. Comput. Chem.* **2006**, *27*, 1415−1428.
(19) Rose, K.; Shadle, S. E.; Eidsness, M. K.; Kurtz, D. M., Jr.; Scott, R. A.; Hedman, B.; Hodgson, K. O.; Solomon, E. I. *J. Am. Chem. Soc.* **1998**, *120*, 10743−10747.
(20) (a) Rose, K.; Shadle, S. E.; Glaser, T.; de Vries, S.; Cherepanov, A.; Canters, G. W.; Hedman, B.; Hodgson, K. O.; Solomon, E. I. *J. Am. Chem. Soc.* **1999**, *121*, 2353−2363. (b) Anxolabéhère-Mallart, E.; Glaser, T.; Frank, P.; Aliverti, A.; Zanetti, G.; Hedman, B.; Hodgson, K. O.; Solomon, E. I. *J. Am. Chem. Soc.* **2001**, *123*, 5444−5452.
(21) Glaser, T.; Bertini, I.; Moura, J. J. G.; Hedman, B.; Hodgson, K. O.; Solomon, E. I. *J. Am. Chem. Soc.* **2001**, *123*, 4859−4860.
(22) Dey, A.; Okamura, T.-A.; Ueyama, N.; Hedman, B.; Hodgson, K. O.; Solomon, E. I. *J. Am. Chem. Soc.* **2005**, *127*, 12046−12053.
(23) Farmer, P. J.; Reibenspies, J. H.; Lindahl, P. A.; Darensbourg, M. Y. *J. Am. Chem. Soc.* **1993**, *115*, 4665−4674.

Fitting Procedures. Pre-edge features were fit by pseudo-Voigt line shapes (sums of Lorentzian and Gaussian functions) using the *EDG_FIT* software.[24] This line shape is appropriate, as the experimental features are expected to be a convolution of a Lorentzian transition envelope and a Gaussian line shape imposed by the beam line optics.[25,26] A fixed 1:1 ratio of Lorentzian to Gaussian contribution successfully reproduced the pre-edge features and was kept fixed during the fitting procedure. The rising edges were also fit with the same pseudo-Voigt line shapes. Fitting requirements included reproducing the data and its second derivative, using the minimum number of peaks. The intensity of a pre-edge feature (peak area) was calculated using the expression intensity = 2× amplitude × full-width-at-half-maximum (fwhm). The fwhm value is between 0.45 and 0.5 for each peak. The reported intensity values for the model complexes are an average of all of the accepted pre-edge fits, typically 5−6 (which differed from each other by less than 3%). The fitted intensities were converted to percent S_{3p} character using the pre-edge feature of plastocyanin as a reference (where 1.01 units of intensity, obtained using this program, corresponded to 38% S_{3p} character), as the Z_{eff} value on the S atom of the thiolate ligand will not change significantly between the Cu−S active site of plastocyanin and the Ni−S complexes studied here.

DFT Calculations. All calculations were performed on dual-CPU Pentium Xeon 2.8 GHz work stations. Geometry optimizations were performed using the BP86[27,28] functional in *the Gaussian 03* program[29] employing a 6-311g* basis set on the Fe,Ni,S and N atoms and a 6-31g* basis set on the C and H atoms. Single point calculations were performed using 6-311++g** basis set on all atoms for wavefunction and population analysis. A polarizable continuum[30] solvation model (acetonitrile as solvent) was used for energy calculations. For calculations of ionization energies (IE's), the geometries were optimized for both oxidation states and the energy of a free electron was accounted for (4.43 eV).[31] The molecular orbitals were plotted using *MOLDEN*, and the Mulliken[32] population analyses were performed using the *PyMOlyze*[33] program.

Results

The S K-edge XAS spectrum of Ni(DACO) is shown in Figure 2A (black). The spectrum has a sharp feature at 2470.8 eV (Table 1, first row), which is assigned to the $RS_{1s} \rightarrow Ni_{3d}$ *pre-edge* transition. The intensity of the pre-edge transition is directly proportional to the S_{3p} orbital mixing in the acceptor Ni_{3d} lowest unoccupied molecular orbital (LUMO) (eq 1) of this square-planar Ni^{II} complex, i.e., Ni−S bond covalency. The pre-edge can be fit with a single peak, and the intensity obtained is 1.25 units; that corresponds to 46% S_{3p} character (Table 1, first row) in the acceptor Ni_{3d} orbital. Note that the pre-edge feature includes two degenerate transitions, one from each sulfur. Thus, 46% S_{3p} character implies that each thiolate contributes 23% S_{3p} character to the wavefunction. The *rising-edge* at ~2472.8 eV (Table 1, first row) is assigned to the $RS_{1s} \rightarrow RS_{C-S\ \sigma^*}$ transition.[34] The S K-edge spectrum of Ni(DACO) in H_2O solution (Figure 2A, black, dashed) shows that the pre-edge shifts to 2471.0 eV (Table 1, second row, a ~0.2 eV increase) but shows no decrease in intensity. This energy shift could be a result of solvent H-bonding or axial coordination of the solvent molecules to the Ni center. The XAS data of Ni(DACO) dissolved in CH_3CN solution (Figure 2A, red),

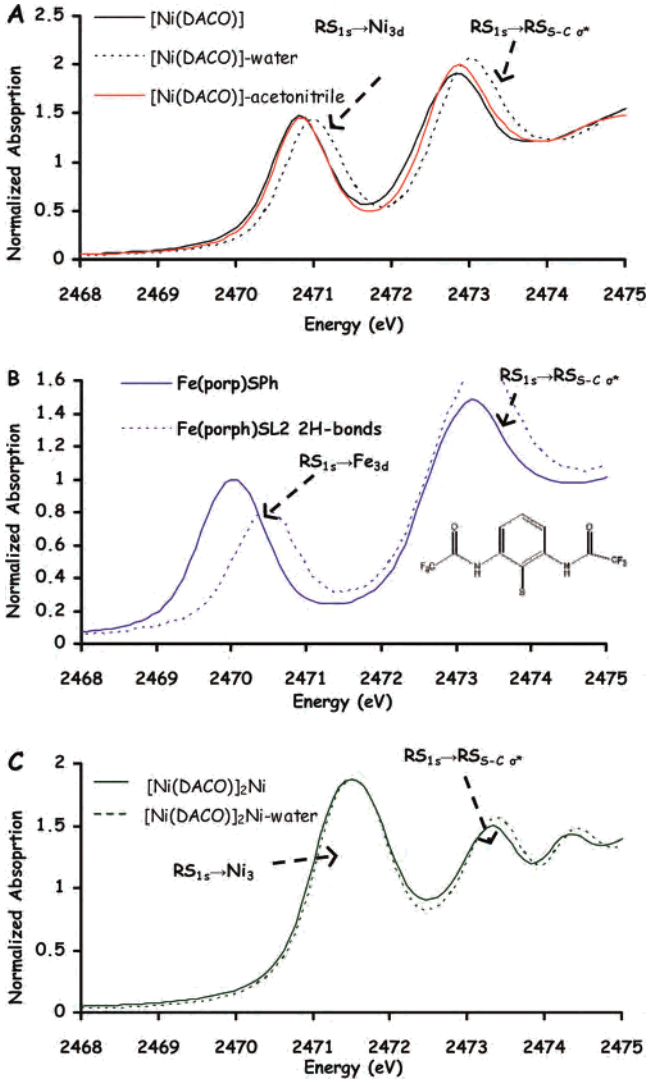

Figure 2. S K-edge XAS spectrum of (A) [Ni(DACO)] as a solid (black), aqueous solution (dotted black), and acetonitrile solution (red); of (B) Fe(porp)SPh (blue) and Fe(porp)SL2 (dashed blue, SL2 refers to 2,6-bis-(trifluoroacetamide)−thiophenol as shown in inset) adapted from ref 22; and of (C) $[Ni(DACO)]_2Ni$ as a solid (green) and in aqueous solution (dashed green).

(24) George, G. N. *EXAFSPAK* and *EDG_FIT*; Stanford Synchrotron Radiation Laboratory, Stanford Linear Accelerator Center, Stanford University: Stanford, CA, 2000.
(25) Agarwal, B. K. *X-ray Spectroscopy*; Springer-Verlag: Berlin, 1979; pp 276 ff.
(26) Tyson, T. A.; Roe, A. L.; Frank, P.; Hodgson, K. O.; Hedman, B. *Phys. Rev. B: Condens. Matter Mater. Phys.* **1989**, *39*, 6305−6315.
(27) Becke, A. D. *Phys. Rev. A: At., Mol., Opt. Phys.* **1988**, *38*, 3098−3100.
(28) Perdew, J. P. *Phys. Rev. B: Condens. Matter Mater. Phys.* **1986**, *33*, 8822−8224.
(29) Frisch, M. J. et al. *Gaussian 03*, revision C.02; Gaussian, Inc.: Wallingford, CT, 2004. Complete citation is provided in the Supporting Information.
(30) Miertus, S.; Scrocco, E.; Tomasi, J. *Chem. Phys.* **1981**, *55*, 117−129.
(31) Han, Wen-Ge; Lovell, T.; Noodleman, L. *Inorg. Chem.* **2002**, *41*, 205−218.
(32) Mulliken, R. S. *J. Chem. Phys.* **1955**, *23*, 1833−1840.
(33) Tenderholt, A. L. *PyMOlyze*, version 1.1; Stanford University: Stanford, CA. http://pymolyze.sourceforge.net.
(34) Dey, A.; Chow, M.; Taniguchi, K.; Lugo-Mas, P.; Davin, S.; Maeda, M.; Kovacs, J. A.; Odaka, M.; Hodgson, K. O.; Hedman, B.; Solomon, E. I. *J. Am. Chem. Soc.* **2006**, *128*, 533−541.

Table 1. XAS Results

complex	pre-edge intensity	S_{3p} (%)	pre-edge energy	rising-edge energy
Ni(DACO)	1.25 ± 0.01	46 ± 1	2470.8 ± 0.1	2472.8 ± 0.1
Ni(DACO) + H_2O	1.25 ± 0.01	46 ± 1	2471.0 ± 0.1	2473.0 ± 0.1

Table 2. DFT-Calculated Geometry and Wavefunction

	geometric parameters (average)				wavefunction (summed overall unoccupied M_{3d} orbitals)		
model	M−S[a]	M−N[a]	S−O[a]	S−H−O[b]	M_{3d} (%(	S_{3p} (π,σ) (%)	N_{2p} (%)
Ni(DACO)	2.17 (2.17)	2.00 (1.98)			47	0, 38	11
Ni(DACO) + $2H_2O$	2.18	1.99	3.33	165	47	0, 38	12
FePSMe	2.30	2.09			359	32, 22	59
FePSMe + H2O	2.31	2.09	3.36	151	361	27, 22	60

[a] Units in Å. [b] Units in degrees.

however, does not show the energy shift observed in the H_2O solution data. This eliminates the possibility of solvent coordination as a cause for the observed pre-edge energy shift and indicates that this is, in fact, a result of solvent H-bonding.[35]

The lack of intensity change on H-bonding is in contrast to the results obtained for a series of ferric heme thiolate complexes where the pre-edge intensity decreased from 1.3 to 1.01 units upon introducing two H-bonds to the thiolate (Figure 2B).[22] There was also a 0.5 eV shift in the pre-edge energy which, however, was found to be a result of the electron-withdrawing effect of the substituents and not H-bonding.

The S K-edge XAS spectrum for the bridged complex $[Ni(DACO)]_2Ni$ (Figure 2C, green) shows a broad pre-edge at 2471.6 eV.[36] The pre-edge in this case represents transitions from four thiolate sulfurs to the three Ni centers. The data do not allow individual resolution of these contributions. The data for the aqueous solution of this complex (Figure 2C, dashed green) shows no resolvable effect on the energy or the intensity relative to the solid. The lack of any effect of H-bonding in this complex contrasts with the behavior of Ni(DACO) (Figure 2A). This difference originates from the additional Ni−S bonding interactions in $(NiDACO)]_2Ni$ considered below.

A. Analysis. The S K-edge XAS data of the Ni(DACO) complex show different behavior from those of the high-spin Fe^{III} heme thiolate complex in ref 22. While the pre-edge intensity was reduced upon H-bonding in the Fe^{III} case, there is no resolvable change in intensity in the Ni^{II} case. The only resolvable change is the shift of the pre-edge to higher energy. DFT calculations were performed to understand this difference.

A1. DFT Calculations on Ni^{II}−Thiolate. The DFT calculations of the Ni(DACO) complex were performed without and with H-bonding. The H-bonding was simulated by adding H_2O molecules in the vicinity of the Ni(DACO) complex.[37] The optimized bond distances for Ni(DACO) (Table 2, first row) are in reasonable agreement with its reported crystal structure (Table 2, first row, in parentheses).[38] The calculations indicate that both without and with H-bonding the Ni $3d_{x^2-y^2}$ orbital is the LUMO and that it has strong σ antibonding interactions with the N_{2p} and the S_{3p} orbitals (Figure 3; the complete MO diagram is provided in Supporting Information Figure S1). The calculated wavefunction has a total 38% S_{3p} character (19% each) in the acceptor Ni $3d_{x^2-y^2}$ orbital compared with the 46% character observed experimentally. One possible source of this difference is a final state effect. We have thus calculated the $S1s^1\cdots Ni3d^9$ excited final state. This shows that the valence-electron density has been redistributed such that the Ni character increased (by 4%) and the character of the S without the 1s hole also increased (by 4%). The effect of this is to redistribute some of the Koopmans' state into the relaxed final state. We have calculated this using the sudden approximation, which is appropriate for this high-energy region, and find that this has the effect of a small decrease (<20%) of pre-edge intensity, which gets redistributed into shakeup peaks at energy greater than 4 eV, which will overlap the edge. This electronically relaxed final state slightly increases the deviation of the experimental ground-state covalency calculated with DFT.

The calculations on the H-bonded Ni(DACO) complex show that both the Ni−S bond length and the Ni−S covalency were not altered upon H-bonding (Table 2, second row), thus reproducing the experimental data. The calculations also indicate that as a result of the interaction with the water molecules, the S_{1s} orbitals of the H-bonded thiolates, in Ni(DACO), are stabilized by 0.2 eV relative to the S_{1s} orbitals of the non-H-bonded thiolates, while no such shift is observed in the acceptor Ni_{3d} orbital. This stabilization of the donor 1s orbital relative to the acceptor Ni $3d_{x^2-y^2}$ orbital

(35) This is also supported by ^1H NMR (data not shown) on this complex in CD_3CN and D_2O solvents.

(36) Note that this pre-edge has contributions from three Ni^{II} centers and four thiolates.

(37) Both the two and four H_2O water molecules were added near the complex and gave the same electronic structure description. Also, two different starting structures were used for these optimizations, one where the water molecules were above the S−Ni−S plane and another where they were in the plane. Both starting structures optimized to the same final geometry presented in the text. Restricting the water molecules to stay in the S−Ni−S plane resulted in a structure that was 2.5 kcal/mol higher in energy.

(38) Darensbourg, M. Y.; Font, I.; Mills, D. K.; Pala, M.; Reibenspies, J. H. *Inorg. Chem.* **1992**, *31*, 4965−4971.

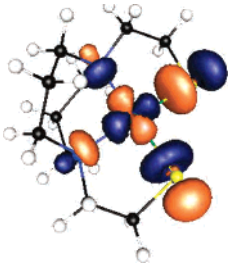

Figure 3. Contour of the Ni $3d_{x^2-y^2}$ acceptor LUMO in Ni(DACO).

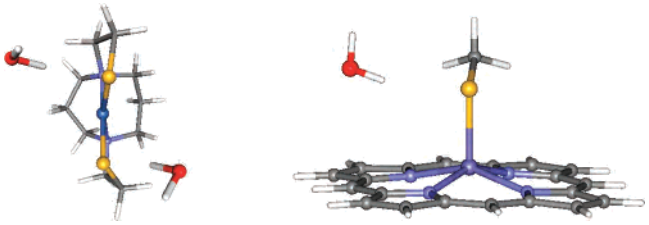

Figure 4. Optimized geometries of the H-bonded Ni(DACO) (left) and FePSMe (right).

is consistent with the 0.2 eV upshift of the pre-edge transition. Note that there is a 0.01 Å decrease in the average Ni−N bond length upon H-bonding. However, this decrease does not significantly affect the ground-state wavefunction of the Ni complex (Table 2, rows 1 and 2).

The optimized geometry of the H-bonded Ni(DACO) complex (Figure 4, left) indicates that the water molecules align to interact with the nonbonding π donor orbitals (perpendicular to the S−Ni−S plane) in preference to the σ donor orbitals (in the S−Ni−S plane).[40] This model of H-bonding is supported by the lack of a solvent H-bond effect on the S K-edge XAS spectrum of the bridged complex [Ni(DACO)]$_2$Ni (Figure 2C) where the two available S_{3p} π donor orbitals in Ni(DACO) are coordinated to the bridging Ni^{II} ion (Figure 1) forming a σ bond.[39] Thus, there is no lone pair available for H-bonding to H_2O.

A2. DFT on Fe^{III}−Thiolate. Previous S K-edge results on high-spin Fe^{III}(porphyrinato)thiolates showed a significant decrease of pre-edge intensity, i.e., Fe−S bond covalency. There was, however, a 0.5 eV increase in pre-edge energy on H-bonding. Calculations on a model with an electron-withdrawing group (EWG) but not an H-bonding substituent (ester) showed that this shift was not due to H-bonding but to a inductive effect of the EWG, which shifted charge density from the C−S σ bond.[22] Similar results are obtained here in the DFT calculations on Fe^{III}(porphyrinato)(methylthiolate) (FePSMe) complexes. The Fe−S bond elongates by only 0.01 Å, and the Fe−S π bond covalency decreases by 5% upon H-bonding (Table 2, rows 3 and 4). These calculations also show that the stabilization of the S_{1s} orbital (due to dipolar interaction with H_2O) is associated with an equal stabilization of the Fe_{3d} orbitals (due to an increased Z_{eff} value due to decreased covalency), and thus there is no effect on the pre-edge energy upon H-bonding in this case. The calculated behavior of the high-spin Fe^{III}−thiolate complex is different from the results obtained for the low-spin Ni−thiolate complex, where upon H-bonding there is no change in Ni−S bond covalency but a shift to higher energy.

Table 3. Calculated Ionization Energies and F^- Binding Energies

model	IE[a] (V)	Q_M[b] (NPA)	ΔBE_{M-F}[c] (kcal/mol)
Ni (DACO)	−2.050	0.50	0
Ni(DACO) + $2H_2O$	−2.035	0.51	−2
FePSMe	−0.936	1.33	0
FePSMe + H_2O	−0.773	1.35	−10

[a] IE refers to ionization energy. [b] Q_M refers to the natural charge on metal. [c] ΔBE_{M-F} refers to the metal−fluoride bonding energy

Discussion

H-bonding effects on M−S bond covalency are different in high-spin Fe^{III} relative to those of square-planar Ni^{II}−thiolate systems. Although in both cases the H-bonds are oriented along the π donor orbitals, in the case of Fe^{III}, this orbital is involved in bonding to the half-occupied Fe_{3d} orbitals, while in the case of Ni^{II}, the thiolate π orbital is nonbonding, as the d-π orbitals are filled. Therefore, H-bonding to the π donor orbital of a thiolate weakens the π bonding in Fe^{III} but has no effect on the σ bonding in Ni^{II}.

The orientations of the H_2O molecules suggest that the π donor orbitals are better H-bond acceptors than the σ donor orbitals.[40] This preferential H-bonding reflects the higher electron density in the π donor orbitals. The σ orbital of the thiolate has better overlap due to its orientation and covalently donates more charge to the metal orbitals. The π orbital thus retains more residual electron density for H-bonding.[41] This predominantly π-based H-bonding interaction in M−S systems is "active" in the Fe^{III}−thiolate system as it weakens the Fe−S π bond. However, in the case of the low-spin Ni^{II}−thiolate, the H-bonding is "passive", as this interaction with the nonbonding π donor orbitals does not affect the Ni−S bond covalency.

In the active system, H-bonding lowers the thiolate donation to the metal. This shifts the reduction potential to a more positive value and increases its Lewis acidity. The calculated ionization energies (solvent corrected and free energy of electron subtracted) for the $Fe^{III/II}$PSMe complex indicate that one active H-bond shifts the $Fe^{III/II}$ potential in FePSMe by +163 mV (Table 3). This effect can be expected to be smaller in a passive system. Similar calculations on Ni(DACO) indicate that even two passive H-bonds shift the $Ni^{II/I}$ potential by only +15 mV (Table 3). The Lewis acidity is estimated from the natural population analysis (NPA) charge on the metal center without and with H-bonding. In the case of passive H-bonding, there is a 0.01 e change in

(39) Geometry-optimized DFT calculations were performed on Ni[Ni(DACO)]$_2$Ni with and without H-bonding from H_2O. The results show that the average S−O distance is 3.5 Å and the average S−H−O angle is 100° in Ni[Ni(DACO)]$_2$Ni + $4H_2O$ relative to 3.3 Å and 175° in Ni(DACO) + $2H_2O$. This indicates that the H-bonding in Ni[Ni(DACO)]$_2$Ni is weak, consistent with experimental results.

(40) This is also indicated in the calculated H-bonding energy, which is −2.6 kcal/mol and −1.9 kcal/mol for π and σ orientations, respectively.

(41) The total donation from the thiolate σ donor orbital into the Fe_{4p} and Fe_{4s} orbitals in FePSMe is calculated to be 13% in addition to the 22% donation to the Fe_{3d} orbital. The π donor orbital only donates 20% to the Fe_{3d} orbital. Thus, the total donation from the σ donor orbital is higher.

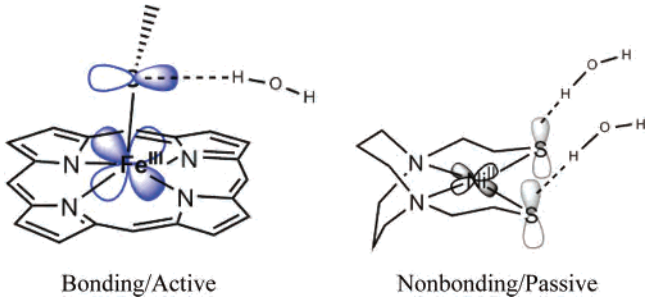

Figure 5. Schematic representation of active (left) and passive (right) H-bonds.

the charge of the metal,[42] while there is an increase of 0.02 e in the active case (Table 3). This change of Lewis acidity is reflected in the enhanced F^- binding energy (calculated to be 10 kcal/mol for FePSMe and 2 kcal/mol for Ni(DACO) in the gas phase, Table 3) to the vacant axial position of the complex with an active H-bond.

In summary, H-bonds to a thiolate ligand can be considered active or passive based on the involvement of the H-bond acceptor orbital in thiolate−metal bonding (Figure 5). In the active case, the H-bond (Figure 5, left) acceptor orbital is involved in M−S π bonding and H-bonding significantly alters the electronic structure and reactivity of the metal center. However, if the H-bond acceptor orbital is not a thiolate donor orbital (i.e., there in no π bonding), then it is passive in nature (Figure 5, right) and does not affect M−S covalency or tune reactivity.

Acknowledgment. This research was supported by NIH Grants 0446304 (E.I.S.) and RR-01209 (K.O.H.) and NSF Grant CHE 06-11695 (M.D.). SSRL operations are supported by the Department of Energy, Office of Basic Energy Sciences. The SSRL Structural Molecular Biology Program is supported by the National Institutes of Health, National Center for Research Resources, Biomedical Technology Program, and by the Department of Energy, Office of Biological and Environmental Research. Dr. Diego Del Rio is acknowledged for helpful discussions.

Supporting Information Available: Optimized geometries of the Ni and Fe complexes. This material is available free of charge via the Internet at http://pubs.acs.org.

IC7006292

(42) Carpenter, J. E.; Weinhold, F. *J. Mol. Struct. (THEOCHEM)* **1988**, *169*, 41.